Talanta 83 (2010) 130–138

Contents lists available at ScienceDirect

Talanta

journal homepage: www.elsevier.com/locate/talanta

A batch modelling approach to monitor a freeze-drying process using in-line Raman spectroscopy

Mafalda Cruz Sarraguça[a], Thomas De Beer[b], Chris Vervaet[c], Jean-Paul Remon[c], João Almeida Lopes[a,*]

[a] REQUIMTE, Departamento de Química, Faculdade de Farmácia, Universidade do Porto, Rua Aníbal Cunha 164, 4099-030 Porto, Portugal
[b] Laboratory of Pharmaceutical Process Analytical Technology, Ghent University, Harelbekestraat 72, B-9000 Ghent, Belgium
[c] Laboratory of Pharmaceutical Technology, Ghent University, Harelbekestraat 72, B-9000 Ghent, Belgium

ARTICLE INFO

Article history:
Received 1 July 2010
Received in revised form 16 August 2010
Accepted 26 August 2010

Keywords:
Freeze-drying
D-Mannitol
Batch process monitoring
Process analytical technology
Multi-way analysis
PLS
PARAFAC

ABSTRACT

Freeze-drying or lyophilisation is a batch wise industrial process used to remove water from solutions, hence stabilizing the solutes for distribution and storage. The objective of the present work was to outline a batch modelling approach to monitor a freeze-drying process in-line and in real-time using Raman spectroscopy. A 5% (w/v) D-mannitol solution was freeze-dried in this study as model. The monitoring of a freeze-drying process using Raman spectroscopy allows following the product behaviour and some process evolution aspects by detecting the changes of the solutes and solvent occurring during the process. Herewith, real-time solid-state characterization of the final product is also possible.

The timely spectroscopic measurements allowed the differentiation between batches operated in normal process conditions and batches having deviations from the normal trajectory. Two strategies were employed to develop batch models: partial least squares (PLS) using the unfolded data and parallel factor analysis (PARAFAC). It was shown that both strategies were able to developed batch models using in-line Raman spectroscopy, allowing to monitor the evolution in real-time of new batches. However, the computational effort required to develop the PLS model and to evaluate new batches using this model is significant lower compared to the PARAFAC model. Moreover, PLS scores in the time mode can be computed for new batches, while using PARAFAC only the batch mode scores can be determined for new batches.

1. Introduction

Freeze-drying, also called lyophilisation, is a three stages drying process used to convert solutions of (heat-)labile materials into solids of sufficient stability for distribution and storage [1]. The initial stage is a freezing step in which water is converted into ice, and the solutes are crystallized or transformed into an amorphous system. The shelf temperature in the freezing state is set to ensure that the product is cooled bellow the glass transition temperature. The second stage is a primary drying step in which the ice is sublimated under vacuum. The temperature during the primary drying is increased (but kept under the collapse temperature) to supply energy for ice sublimation. The process ends with a secondary drying step in which all the unfrozen water is removed by desorption and/or in which hydrate water is removed [2]. Freeze-drying is a widely used process for the preservation of microorganisms, food items, biological products and pharmaceuticals [3–6]. In the pharmaceutical industry, the process provides improved stability, and/or desired physicochemical properties, such as enhance dissolution rates and bioavailability [6,7].

Real-time monitoring of freeze-drying processes is essential to reduce costs and to improve process knowledge and efficiency. Freeze-drying cycles are in many cases set up by trial and error, herewith only focussing on the final product quality [8]. During the last decades, several methods based on product temperature and pressure measurements were developed to monitor freeze-drying processes [7–9]. However, these methods do not allow the in-line monitoring of all critical process aspects (e.g., product behaviour).

In recent years, several methods based on the concept of process analytical technology (PAT) have emerged in the pharmaceutical industry, the majority of them using spectroscopic techniques [10]. Spectroscopic tools have several advantages over other analytical methods such as high performance liquid chromatography (HPLC): they can be non-invasive and non-destructive and can be used in-line hence providing real-time information. The application of near infrared spectroscopy (NIRS) and Raman spectroscopy does not only supply information about the chemical and physical properties of the final product (e.g., physical state, polymorphism), but also about the chemical and physical changes occurring over time. In previous studies, Raman spectroscopy and NIRS [2,3,9,11,12] were

* Corresponding author. Tel.: +351 222078994; fax: +351 222078961.
E-mail address: joaolopes@ff.up.pt (J.A. Lopes).

0039-9140/$ – see front matter © 2010 Elsevier B.V. All rights reserved.
doi:10.1016/j.talanta.2010.08.051

evaluated as potential tools for the in-line and real-time monitoring of freeze-drying processes. Using these methods, the determination of some process stage end-points as well as the chemical/physical characterization of the product were achieved. These studies were mainly focussed on process improvement and the detection of process occurrences (e.g., physical state transformations) over time. However, and since freeze-drying is a batch wise process, also the batch-to-batch variation has to be addressed. The differentiation between good and bad batches in the early process phase is a major concern in the pharmaceutical industry since batch-to-batch variability can be unpredictable [13]. The unpredictability of batch variation can lead to quality problems in the final product (e.g., variability in residual moisture content).

The aim of this study was not to focus on the critical freeze-drying process aspects which can be detected using in-line Raman spectroscopy, as this was done previously [9,12]. The objective of this work is to show how freeze-drying process fingerprints obtained by continuous in-line Raman measurements can be used to model reference freeze-drying processes (i.e., development of batch models) allowing to evaluate in real-time whether future new batches are proceeding as the desired reference processes. A 5% (w/v) D-mannitol solution was used as model to freeze-dry [14].

Multi-way models have been recognized as useful tools for monitoring batch data since they improve the process understanding and summarize the process behaviour in a batch wise manner. Multi-way principal component analysis (MPCA) and multi-way partial least squares (MPLS) were used to monitor batch wise processes, such as for example, fluid bed granulation [13,15]. Other multi-way methods such as parallel factor analysis (PARAFAC) and Tucker 3 were also used to monitor batches processes, such as wheat growing experiments using NIRS and polymerization processes [16,17]. In this study PLS and PARAFAC were the employed batch modelling strategies. In this particular case, PLS and not MPLS was used in the work. The data was unfolded and regular PLS was performed on the data, it is important to refer that regular PLS and MPLS algorithms are quite distinct [18].

A set of nominal batches obtained in normal operational conditions (NOC) were used to develop the batch (calibration) models. New batches were projected onto these models to detect any deviation from normal batch trajectories.

1.1. Data analysis

The data obtained from the freeze-drying processes were organized in a three-way array $\underline{\mathbf{X}}$ ($I \times J \times K$) with I batches, J variables (number of spectral variables) and K time points. The PLS was performed using SIMCA P+ 12.01 (Umetrics AB, Umeå, Sweden). PARAFAC modelling was performed using PLS toolbox version 3.5 in Matlab, version 6.5 release 13 (MathWorks, Natick, MA, USA).

1.2. PLS

To develop the PLS model, unfolding of the three-way array was done preserving the variable direction, creating a new mode combining the batch and time mode (M=IK). The row m of the matrix $\mathbf{X}$ has the spectrum corresponding to time point k for the batch i. The dependent variable vector, $\mathbf{Y}$, used for the partial least squares (PLS) regression, has a length equal to M and represent batch duration. By performing PLS regression using time as the dependent variable, the individual observations can be evaluated over time and batch maturity can be predicted. Moreover, by preserving the variable direction, the typical tendency of a batch being operated in NOC, can be followed. The number of PLS components was set by cross-validation using the approach described by Eastment and Krzanowski [19]. To monitor new batches, and compare their trajectory with the NOC batches, control charts are developed. After PLS modelling, a score matrix is obtained ($M \times T$), in which T is the number of latent variables used to fit the PLS model. To create the control charts, the scores matrices are rearranged to produce "T" matrices, one for each latent variable from the PLS model. Row-wise, each of those matrices have dimension ($I \times K$). From each of these matrices, a vector is estimated ($1 \times K$) with a standard deviation (σ) for the corresponding latent variable over the K time points. The control limits are set in as $\pm 3 \times \sigma$. The essence of this reordering principle is that, for each component of the PLS model, an average trajectory with upper and lower control limits is obtained. When projecting the new batches into the model the normal development of these batches can be followed, as well as any deviation from it.

Another control chart is the residuals chart showing the unmodelled variation, for each batch. A good batch should evolve in the same way as the reference batches and be below a critical value set at $+3 \times \sigma$, in which the standard deviation is calculated for the average of the residuals from the calibration batches [20].

1.3. PARAFAC

PARAFAC is a method for modelling three-way or higher order data. PARAFAC is a decomposition method that can be compared to the bilinear principal component analysis (PCA) [21]. In the case of a three-way data set the decomposition is performed in three components as can be seen in Eq. (1).

$$x_{ijk} = \sum a_{if} b_{jf} c_{kf} + e_{ijk} \quad (1)$$

In Eq. (1), x_{ijk} is an element of the three-way array $\underline{\mathbf{X}}$; and e_{ijk} is an element of the three-way $\underline{\mathbf{E}}$ of residues. Three ways or modes (a, b and c) are obtained with indices $i = 1,\ldots, I$, $j = 1,\ldots, J$, and $k = 1,\ldots, K$. These indices constitute the loading matrixes $\mathbf{A}$, $\mathbf{B}$ and $\mathbf{C}$. The index f is the number of PARAFAC components. In matrix notation the PARAFAC model can be written as,

$$\mathbf{X}_k = \mathbf{A}\mathbf{D}_k\mathbf{B}^T + \mathbf{E}_k, \quad k = 1, \ldots, K \quad (2)$$

where $\mathbf{D}_k$ is a diagonal matrix holding the k row of $\mathbf{C}$ in its diagonal.

The determination of the number of components is one of the major difficulties of a PARAFAC model. Resampling techniques such as cross-validation or residuals histograms are some of the techniques that can be use to determine the number of PARAFAC components. However, all of them have some disadvantages such as heavy computations involved or the difficulty to determine with assurance the optimum number of components. To overcome the disadvantages, a single diagnostic analysis, called core consistency, that gives clear differences for different models was created. The core consistency is always less or equal to 100%, a good trilinear model can be said to have a core consistency above 90%. Low values of core consistency indicates that elements outside of the super diagonal are significantly different of zero, that the model is not trilinear and a model such Tucker should be used [22].

After the calibration of the PARAFAC model, new batches can be projected onto the model. However, only the loadings of mode 1 (in this case the batch mode) are obtained for the new batches. This fact creates a problem because; no indication on their behaviour over time is obtained. The residuals statistics can be used to obtain a first impression on the new batches. If the sum of squares of the residuals values are higher than the value for the 95% confidence limit, it can be concluded that the predicted batch had some kind of problem during the process. Nonetheless, no information can be retrieved regarding where in time the problem occurred. Batch control charts can be constructed using the Hotellings and residuals statistics by performing the following procedure [17].

Table 1
Freeze-drying conditions for batches in normal operational conditions (calibration batches) and prediction batches 2–4.

Process phase	Calibration batches			Prediction batch 2			Prediction batches 3 and 4		
	Time (min)	Shelf temperature (°C)	Pressure (mb)	Time (min)	Shelf temperature (°C)	Pressure (mb)	Time (min)	Shelf temperature (°C)	Pressure (mbar)
Freezing	0	20	1000	0	20	1000	0	20	1000
	5	2	1000	25	−5	1000	5	2	1000
	25	−5	1000	85	−30	1000	25	−5	1000
	85	−30	1000	145	−45	1000	65	−45	1000
	145	−45	1000				205	−45	1000
Primary drying	165	−45	0.5	190	−45	0.5	215	−15	1
	185	−20	0.5	210	−20	0.5	225	−15	1
	785	−20	0.5	810	−20	0.5	975	−15	1
							977	−15	1
Secondary drying	845	40	0.5	870	25	0.5			
	1085	40	0.5	930	25	0.5			
				960	40	0.5			

- A number PARAFAC models were constructed by cutting the batch duration in expanding time periods, like 0–K/n, 0–$2K/n$,. . . ,0–K time points, in which n is the number of time periods.
- The prediction batches were projected onto each constructed model.
- For each model and for each prediction batches the Hotelling and the residuals sum of squares values were determined.

Batch control charts can be constructed using the Hotelling and the residuals statistics for the different models constructed and setting as control limits the value correspondent to the 95% confidence level. The Hotelling statistic gives an indication on batch variation, or in other words, assesses the statistical significance of the difference between batches. The residuals statistic is an indication how well each batch conforms to the model. Consequently, these parameters can be used as indicators of process consistency.

2. Experimental

2.1. Materials

D-Mannitol (further abbreviated as mannitol) is one of the most used excipients in pharmaceutical freeze-drying. It is generally employed as a bulking agent, crystallizing during lyophilisation, hence providing structural support to the final product.

In this study, 5% (w/v) mannitol solutions (3 ml) were used as model for the freeze-drying process.

2.2. Batches

To develop the batch models, six NOC batches were used (process conditions in Table 1). The batch models were evaluated by running three additional batches having deviating operational conditions, (see Table 1 for process conditions). A NOC batch, not used in the calibration set, was also used to evaluate the developed batch models.

2.3. Process description

The equipment used was an Amsco FINN-AQUA GT4 (GEA, Köln, Germany) freeze-drier. For Raman process monitoring, a Raman probe was built into the freeze-drier chamber. The probe was placed above a vial, hence allowing to monitor the formulation top surface without contact between product and probe. The optical fiber cable of the Raman probe was connected through a gap made in the freeze-drier chamber door [2,9,12].

2.4. Raman spectroscopy

A RamanRxn1 spectrometer (Kaiser Optical Systems, Ann Arbor, MI) equipped with an air-cooled CCD detector (black-illuminated deep depletion design) was used in combination with a fiber optic non-contact probe to monitor the freeze-drying processes. As the Raman probe was directly placed above the product to freeze dry, the glass vial did not interfere with the Raman signal. The laser wavelength was 785 nm (NIR diode laser). All spectra were collected at a resolution of 4 cm^{-1} using a laser power of 400 mW. Data collection and transfer were automated using the HoloGRAMS™ data collection software. A spectrum was collected every 2 min during lyophilisation with 30 s exposures.

3. Results and discussion

Two different Raman spectral regions were used to monitor the freeze-drying processes. Ice produces a Raman signal in the region between 150 cm^{-1} and 250 cm^{-1} while mannitol produces signals between 1000 cm^{-1} and 1170 cm^{-1} [9]. Furthermore, the different polymorphic forms of mannitol can be distinguished in this spectral region. These two spectral regions were used together (in total 901 spectral variables) to develop the batch models. During the freezing step, ice formation can be detected by the appearance of the ice peak at 215 cm^{-1} (Fig. 1a). Shortly after the water solidification, mannitol starts to crystallize (Fig. 1b). During primary drying, the ice is sublimated. The disappearance of the peak at 215 cm^{-1} can be seen during this process step (Fig. 1c). Furthermore, the peaks corresponding to mannitol do not show any visible changes, indicating that no transformations related to mannitol occurred during primary drying (Fig. 1d). The temperature was raised for the secondary drying step to remove the hydrate water (i.e., to convert mannitol hemi-hydrate to an anhydrous form [9]). The Raman signals corresponding to mannitol hemi-hydrate disappear or decrease in intensity and new Raman peaks corresponding to anhydrous mannitol (α form) appear at 1030 cm^{-1} and 1130 cm^{-1} (Fig. 1f).

Raman spectra were collected every 2 min to decrease the computational effort, resulting in a total of 550 spectra per batch. Consequently, the calibration data is arranged in a three-way array $\underline{\mathbf{X}}$ ($I \times J \times K$) of $I = 6$ batches, $J = 901$ spectral variables and $K = 550$ time points.

3.1. Batch modelling – PLS

The unfolding of the three-way array by preserving the variable direction resulted in a matrix $\mathbf{X}$ ($M \times J$) with $M = 3300$ (6 batches with 550 time points) and $J = 901$. Before PLS analysis, the spectra were pre-processed using standard normal variate (SNV) and

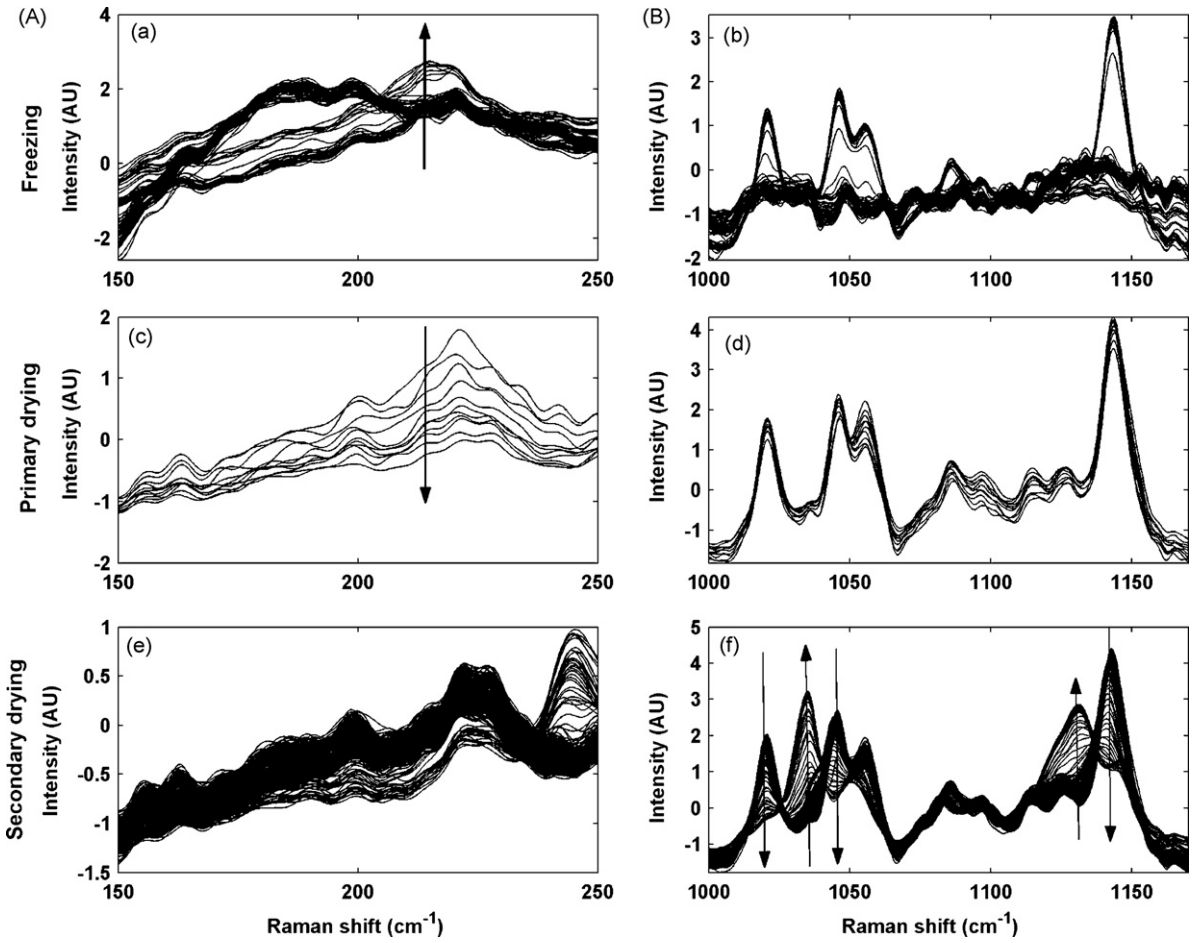

Fig. 1. Raman spectra corresponding to the three process steps for the two studied spectral ranges. (A) Ice signal range and (B) mannitol signal range.

mean centred. A PLS model was developed and cross-validation was performed, resulting in a two component model (cumulative variance of **X** of 0.89 (Table 2)). A three component model did not significantly improved the explained variance (increase of 0.019). Consequently, a two component model was chosen.

Analysing the PLS model loadings (Fig. 2) it can be seen the spectral variations described by each PLS component. The loadings correspondent to the first component are related to the transformations occurred during the freezing and primary drying stages. The section of the loadings that correspond to the ice signal (Fig. 2a) shows the variations that occurred in the band at 215 cm^{-1}. Comparing Fig. 2b with Fig. 1a and d, is clear that the loadings describe the mannitol transformations taking place during the freezing and primary drying stages. The loadings correspondent to the second PLS component (Fig. 2c and d) are related to the transformations occurred during the secondary drying. In the case of the ice signal range (Fig. 2c), the main feature is the appearance of a band at 240 cm^{-1} (Fig. 1e). The loadings correspondent to the mannitol transformation range (Fig. 2d) relate to the appearance and disappearance of bands during the secondary drying (polymorphic transformation). The changes occurring during the process can also be detected analysing the scores evolution over time (Fig. 3). Only the scores of calibration batch 2 are depicted for visualization clarity. The increase of the PLS 1 component scores after 102 min (I) is related to the beginning of the water to ice conversion. Mannitol crystallization can be detected by the increase of the first PLS component scores and the decrease of the second PLS component scores at 122 min (II). The start of the primary drying (A) is not followed by any significant changes in the scores. An increase of the scores for both PLS components at 194 process minutes (III) is attributed to ice sublimation during the primary drying. The beginning of the secondary drying is accompanied by an increase of the scores for both PLS components (B). The reason that the secondary drying can be detected, opposed to the primary drying, is the substantial increase in the temperature (60 °C) in the secondary drying stage. The polymorphic transformation between hemi-hydrate and α mannitol at minute 1038 (IV) can be seen in the increase of the second PLS component scores.

Table 2
PLS results. *A* – PLS component, R^2X – explained sum of squares, Q^2 – the fraction of the total variation that can be predicted by a component, as estimated by cross-validation.

A	R^2X	R^2X (cum)	Q^2 (cum)
1	0.702	0.702	0.472
2	0.185	0.886	0.604
3	0.019	0.906	0.704

After development of the calibration model, the spectra from the prediction batches were projected onto the model. To evaluate these new batches, batch control charts based on the scores (Fig. 4) and residuals (Fig. 5) from the calibration batches were constructed. The scores from the PLS second component were chosen to construct the control charts (Fig. 4) because they show that information during freeze and primary stages as the first component scores, but the information associated with the secondary drying is more visible in the second component as can be seen in Figs. 2d and 3.

Prediction batch 1 was a nominal batch, i.e., a batch produced under NOC. However, when its trajectory was compared to the

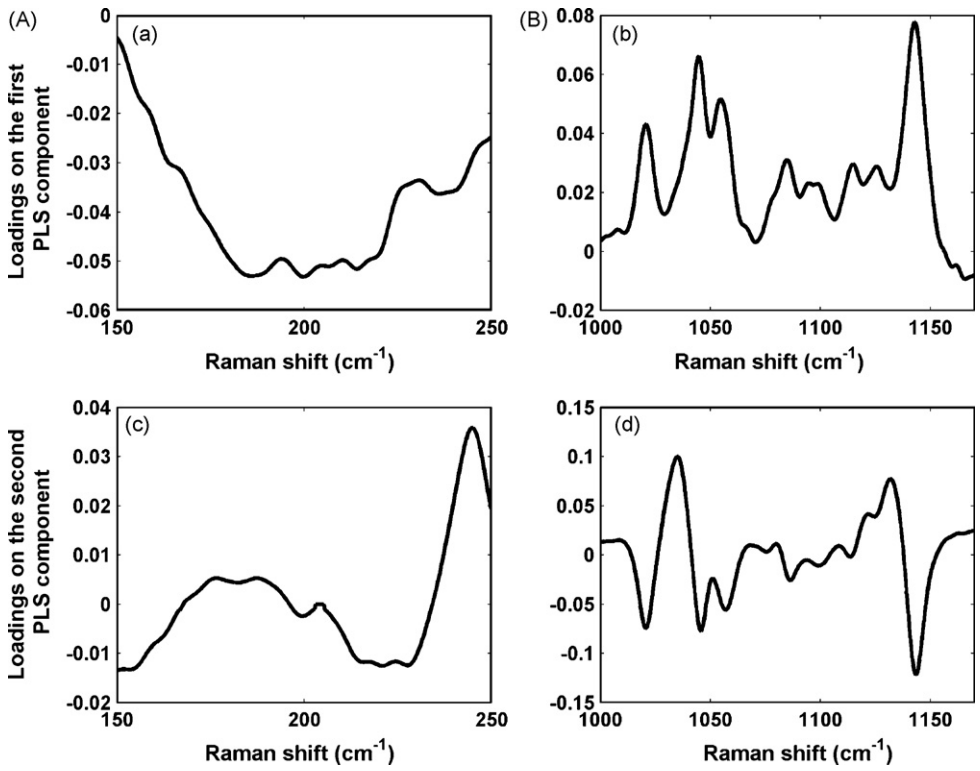

Fig. 2. First and second PLS component loadings for the two studied spectral ranges. (A) Ice signal range and (B) mannitol signal range.

calibration batches trajectories, significant deviations could be detected. In the score batch control chart (Fig. 4) prediction batch 1 is out of control (above the superior limit) until minute 86, indicating some problem in the process conditions or spectra acquisition during that time. Looking to the spectra of prediction batch 1 obtained during the first 86 process minutes (not shown), some abnormalities could be detected. Since the batch trajectory was within the limits the rest of the process, it can be concluded that the initial deviation was related with problems associated with the spectra acquisition. The same conclusion can be drawn by analysing the residuals control chart.

Prediction batches 2–4 were subjected to different process conditions (Table 1). For prediction batch 2, the primary drying step was longer compared to the NOC batches and the shelf temperature

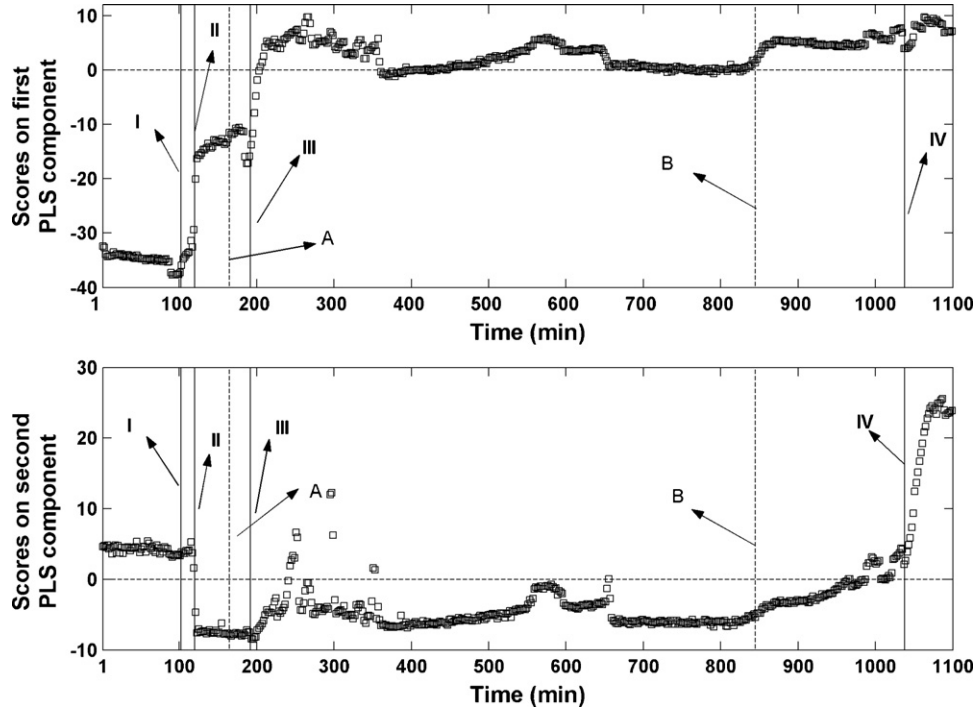

Fig. 3. Evolution over time of the first and second PLS component scores for calibration batch 2. (I) Ice solidification, (II) mannitol crystallization, (III) ice sublimation, (IV) polymorphic transformation, (A) beginning of the primary drying and (B) beginning of the secondary drying.

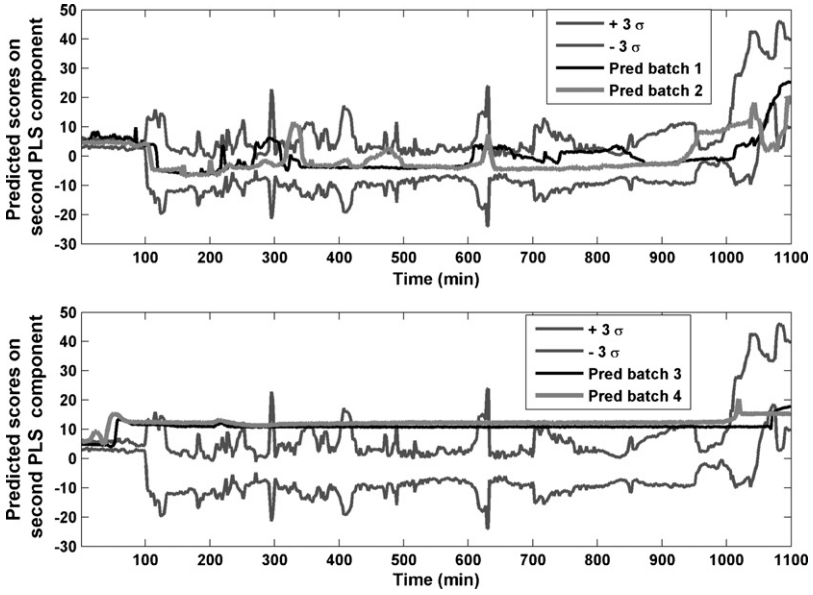

Fig. 4. Evolution over time of the predicted scores for the second PLS component – scores batch control chart.

during the secondary drying stage was first set at 25 °C during the first 100 secondary drying minutes instead of 40 °C. In the score control chart, corresponding to the second PLS component (Fig. 4) a deviation occurred in the end of the process indicating the difference in behaviour of this batch during the secondary drying. In the residuals control chart (Fig. 5) this batch also deviates from the model at the end of the process where the difference in process conditions compared to the NOC batches is more significant.

Prediction batch 3 and 4, have very different process conditions compared to the reference batches (Table 1): the primary drying starts later, the set shelf temperature during primary drying is higher and no secondary drying was done. It is expected that these two bathes are out of trajectory during the entire process time. In fact, the score control charts (Fig. 4) show that the trajectory is completely different. The residuals control chart (Fig. 5) shows that almost the complete trajectory of prediction batches 3 and 4 is above the imposed limit.

3.2. Batch modelling – PARAFAC

To develop the PARAFAC calibration model, a three-way array $\underline{\mathbf{X}}$ ($I \times J \times K$) with $I = 6$ (number of batches), $J = 901$ (number of spectral variables) and $K = 550$ (number of time points) was used. The spectra were pre-processed using SNV and centred before PARAFAC analysis. The number of PARAFAC components was chosen based on the core consistency criterion. For a number of PARAFAC components between 1 and 4 the core consistency and the percentage of explained variance was determined (Table 3). A model with 3 components was chosen with a core consistency value of 94.3% and an explained variance of 44.0%.

The loadings from the third mode (time) of the PARAFAC model can be seen as the average batch trajectory for the calibration batches (Fig. 6). The changes occurring during the process can be seen in the three component loadings. The water to ice conversion around 100 min (I) followed by the mannitol crystallization (II) are

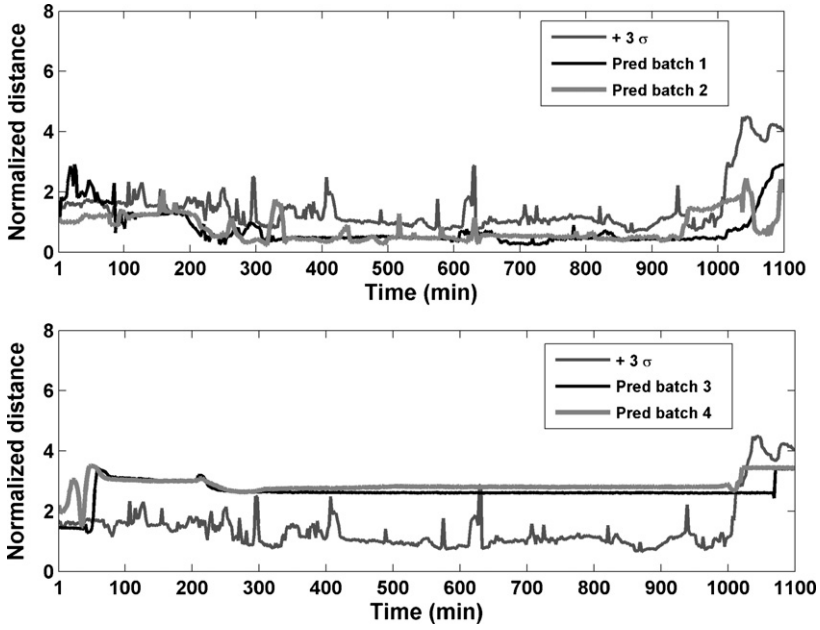

Fig. 5. Evolution over time of the normalized distance correspondent to the PLS residuals for the prediction batches – residuals batch control chart.

Table 3
Variance explained and core consistency for the four first PARAFAC components.

# PARAFAC components	Variance explained (%)	Core consistency
1	24.6	100
2	34.4	100
3	44.0	94.3
4	50.4	65.1

clearly seen in the three component loadings. The ice sublimation occurring around minute 200 (III) can be seen in the first component. The polymorphic transformation occurred at the end of the process (IV) can be followed by an increase in the first component loading and a decrease in the second component loading.

The beginning of the primary drying (A) stage can be seen in the loadings of the first and second component. A decrease in the third component loading around 845 min (B) is an indication of the beginning of the secondary drying.

The loadings for the second mode (spectral variables) and for the three PARAFAC components are shown in Fig. 7. By comparing the loadings with the spectra presented in Fig. 1 it can be concluded (as was the case of the PLS loadings) that they are related to the spectral changes occurred during the three process stages. The loadings correspondent to the first, second and third component are associated with the freezing, primary and secondary drying stages, respectively.

After the calibration model was developed, the four prediction batches were projected onto the model. The residuals sum of squares for the prediction batches (not shown) confirm that batches 3 and 4 are clearly different from the NOC ones. Batches 1 and 2 are above the 99% confidence limit but below the 95% confidence limit. These statistics provide an indication of problematic batches. However, no indication is given in which part of the process trajectory the problem occurred. For this reason, the procedure explained in Section 1.3 was done to get an indication on the process phases during which the problems occurred (Figs. 8 and 9). A total of 22 models were constructed with expanding time periods.

The Hotelling control chart (Fig. 8) shows prediction batch 1 with abnormal behaviour in the first 50 min of the process, which is in accordance with what has already been explained in Section 3.1. However, the residuals (Fig. 9) indicate that this batch is above the control limit until minute 350, and very near to the control limit the rest of the process. Prediction batch 2 is always within the control limit in the Hotelling control chart. Only the last model for this batch is above the control limit in the residuals control chart, indicating that the problem in this batch is in the end of the process as was already discussed above (Section 3.1). Prediction batches 3 and 4 are above the control limit for the first 150 min of the process time according to the Hotelling chart. The plot regarding the residual statistics shows that both batches have a residual value higher than the imposed control limit.

3.3. Batch monitoring with PLS and PARAFAC

The two approaches used to create the batch models gave similar results and conclusions. The conversion of water into ice, mannitol crystallization, ice sublimation at the surface and polymorphic transformation (hydrate removal) were clearly detected by following the scores over time for both methods (Figs. 3 and 6). Batch control charts were constructed and used to evaluate new batches running under normal and non-normal process conditions. Both methods detected that prediction batch 1, thought to be a nominal batch, deviated from the normal trajectory in the beginning of the process (Figs. 4, 5, 8 and 9). Prediction batch 2 was subjected to different process conditions (see Table 1). Hence, it was expected to have a different behaviour, in particularly in the end of the process. The residuals batch control charts (Figs. 5 and 9) showed a few deviations, particularly in the end of the process. For prediction batch 3 and 4, both methods considered them out of limit during the first 150 min (Figs. 4 and 8). The residuals

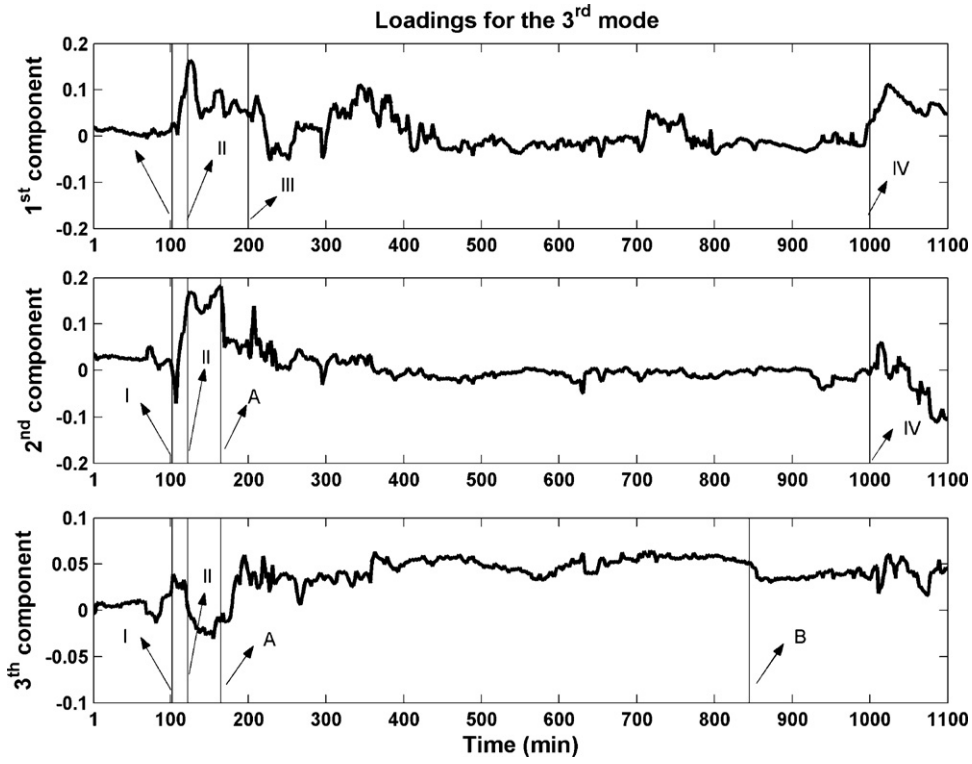

Fig. 6. PARAFAC model loadings for the third mode (time) for the three components. (I) Ice solidification, (II) mannitol crystallization, (III) ice sublimation, (IV) polymorphic transformation, (A) beginning of primary drying, and (B) beginning of secondary drying.

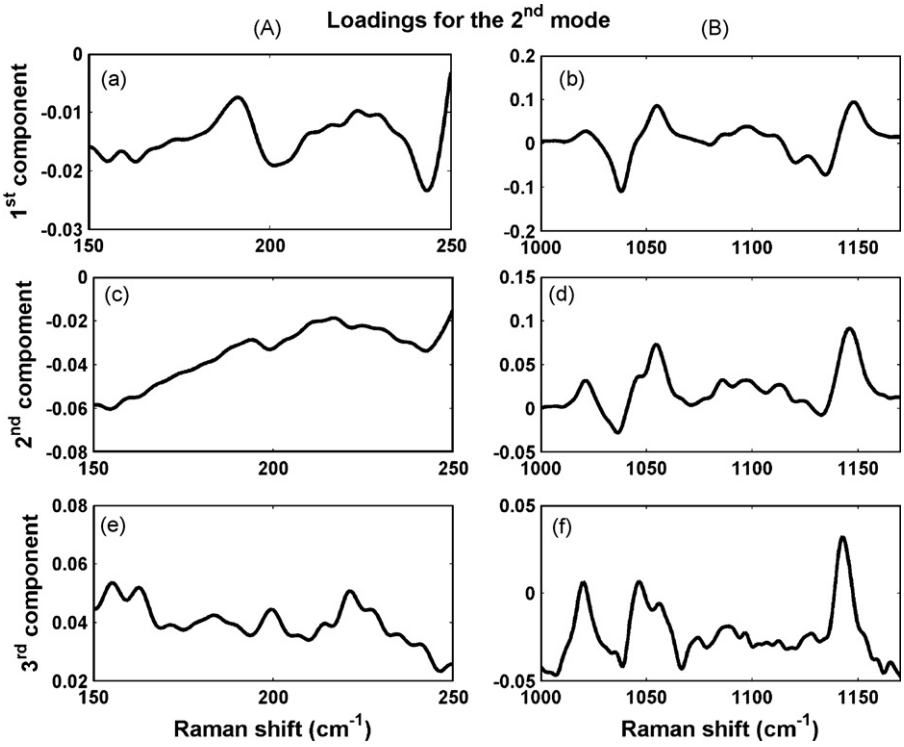

Fig. 7. Loadings for the second PARAFAC mode (spectral variables) for the three components and for the two spectral ranges studied. (A) Ice signal range and (B) mannitol signal range.

control charts for both methods (Figs. 5 and 9) supported these conclusions.

The batch control charts only give information regarding a process disturbance; no information is obtained about the cause of the disturbances. A solution to this problem is the use of contribution plots. By using such plots the contribution of each process variable can be evaluated and control limits can be introduced in the contribution plots. This procedure allows the unveiling of the process variables that show different behaviour compared with the NOC batches [23]. The use of contribution plots is an easy concept when dealing with few process variables, but with spectroscopic data, the use and analysis of these plots is not straightforward. Firstly, the number of variables is very high (wavelengths) and secondly, these variables are highly correlated. To construct contribution plots with spectroscopic data an initial variable reduction should be performed. This possibility is undoubtedly worth of exploration in a future work.

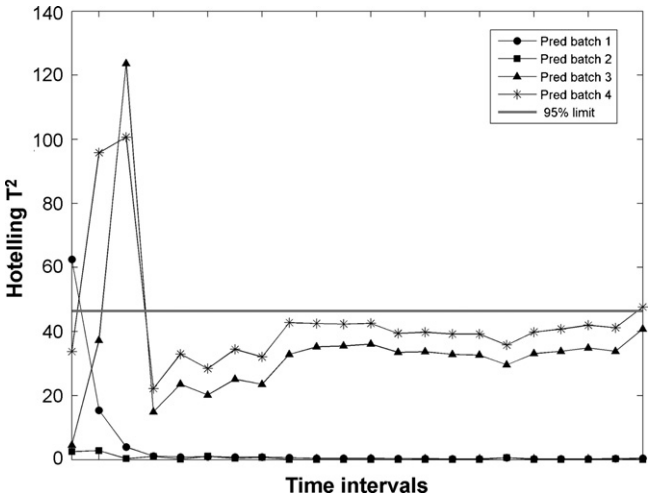

Fig. 8. Hotelling T^2 statistics for the prediction batches as a function of the modelled time intervals for a PARAFAC model with 3 components.

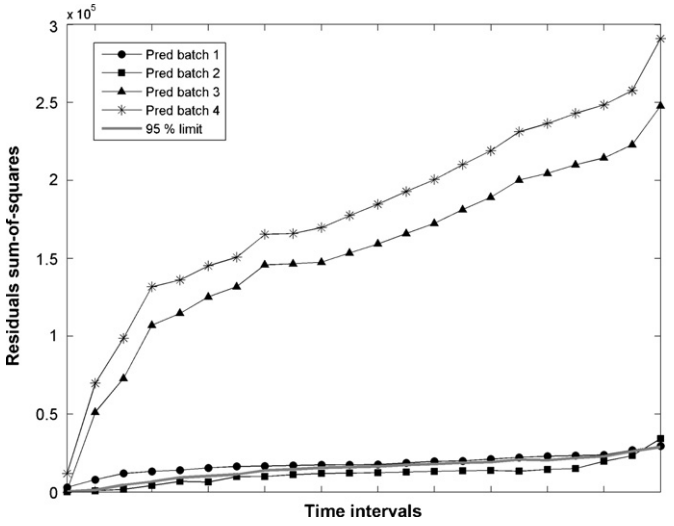

Fig. 9. Residuals statistics for the prediction batches as a function of the modelled time intervals for a PARAFAC model with 3 components.

4. Conclusions

The objective of this work is to show how freeze-drying process fingerprints obtained by continuous in-line Raman measurements can be used to model reference freeze-drying processes (i.e., development of batch models) allowing to evaluate in real-time whether future new batches are proceeding as the desired reference processes. Two chemometric batch modelling approaches were used and tested: PLS and PARAFAC. The main product transformations

occurring during the freeze-drying process can be successfully evaluated during the monitoring of new batches. The PLS and PARAFAC control charts were able to detect non-nominal batches and gave similar results for both methods. It can hence be concluded that PLS and PARAFAC perform equally well. However, the computational effort is less for PLS, compared to PARAFAC, which is important for the real-time evaluation of new batches.

Future work can be performed in order to include contribution plots in the process monitoring.

Acknowledgements

Mafalda C. Sarraguça acknowledges the financial support from the Fundação para a Ciência e Tecnologia (FCT), Portugal (Ph.D. grant, ref: SFRH/BD/32614/2006).

References

[1] M.J. Pikal, in: J. Swarbrick (Ed.), Encyclopedia of Pharmaceutical Technology, Marcel Dekker, New York, 2002, pp. 1807–1833.
[2] T.R.M. De Beer, M. Wiggenhorn, R. Veillon, C. Debacq, Y. Mayeresse, B. Moreau, A. Burggraeve, T. Quinten, W. Friess, G. Winter, C. Vervaet, J.P. Remon, W.R.G. Baeyens, Anal. Chem. 81 (2009) 7639–7649.
[3] M. Brulls, S. Folestad, A. Sparen, A. Rasmuson, Pharm. Res. 20 (2003) 494–499.
[4] V. Rindler, S. Luneberger, P. Schwindke, I. Heschel, G. Rau, Cryobiology 38 (1999) 2–15.
[5] J. Teixeira, Genet. Eng. Biotechnol. News 25 (2005) 52–54.
[6] W. Wang, Int. J. Pharm. 203 (2000) 1–60.
[7] J.S. Liu, Pharm. Dev. Technol. 11 (2006) 3–28.
[8] H. Gieseler, T. Kramer, M.J. Pikal, J. Pharm. Sci. 96 (2007) 3402–3418.
[9] T.R.M. De Beer, M. Alleso, F. Goethals, A. Coppens, Y.V. Heyden, H.L. De Diego, J. Rantanen, F. Verpoort, C. Vervaet, J.P. Remon, W.R.G. Baeyens, Anal. Chem. 79 (2007) 7992–8003.
[10] Y. Roggo, P. Chalus, L. Maurer, C. Lema-Martinez, A. Edmond, N. Jent, J. Pharm. Biomed. Anal. 44 (2007) 683–700.
[11] W.J. Cao, C. Mao, W. Chen, H. Lin, S. Krishnan, N. Cauchon, J. Pharm. Sci. 95 (2006) 2077–2086.
[12] T.R.M. De Beer, P. Vercruysse, A. Burggraeve, T. Quinten, J. Ouyang, X. Zhang, C. Vervaet, J.P. Remon, W.R.G. Baeyens, J. Pharm. Sci. 98 (2009) 3430–3446.
[13] S. Matero, S. Poutiainen, J. Leskinen, S.P. Reinikainen, J. Ketolainen, K. Jarvinen, A. Poso, Chemometr. Intell. Lab. Syst. 96 (2009) 88–93.
[14] R. Chakkittakandy, J.A.W.M. Corver, P.C.M. Planken, J. Pharm. Sci. 99 (2010) 932–940.
[15] T. Kourti, J. Chemometr. 17 (2003) 93–109.
[16] P. Geladi, M. Manley, J. Chemometr. 22 (2008) 247–251.
[17] D.J. Louwerse, A.K. Smilde, Chem. Eng. Sci. 55 (2000) 1225–1235.
[18] R. Bro, A.K. Smilde, S. de Jong, Chemometr. Intell. Lab. Syst. 58 (2001) 3–13.
[19] H.T. Eastment, W.J. Krzanowski, Technometrics 24 (1982) 73–77.
[20] L. Eriksson, E. Johansson, N. Kettaneh-Wold, J. Trygg, C. Wikström, S. Wold, Multi- and Megavariate Data Analysis Part I + Part II, Umetrics AB, Umea, 2001.
[21] R. Bro, Chemometr. Intell. Lab. Syst. 38 (1997) 149–171.
[22] R. Bro, H.A.L. Kiers, J. Chemometr. 17 (2003) 274–286.
[23] J.A. Westerhuis, S.P. Gurden, A.K. Smilde, Chemometr. Intell. Lab. Syst. 51 (2000) 95–114.